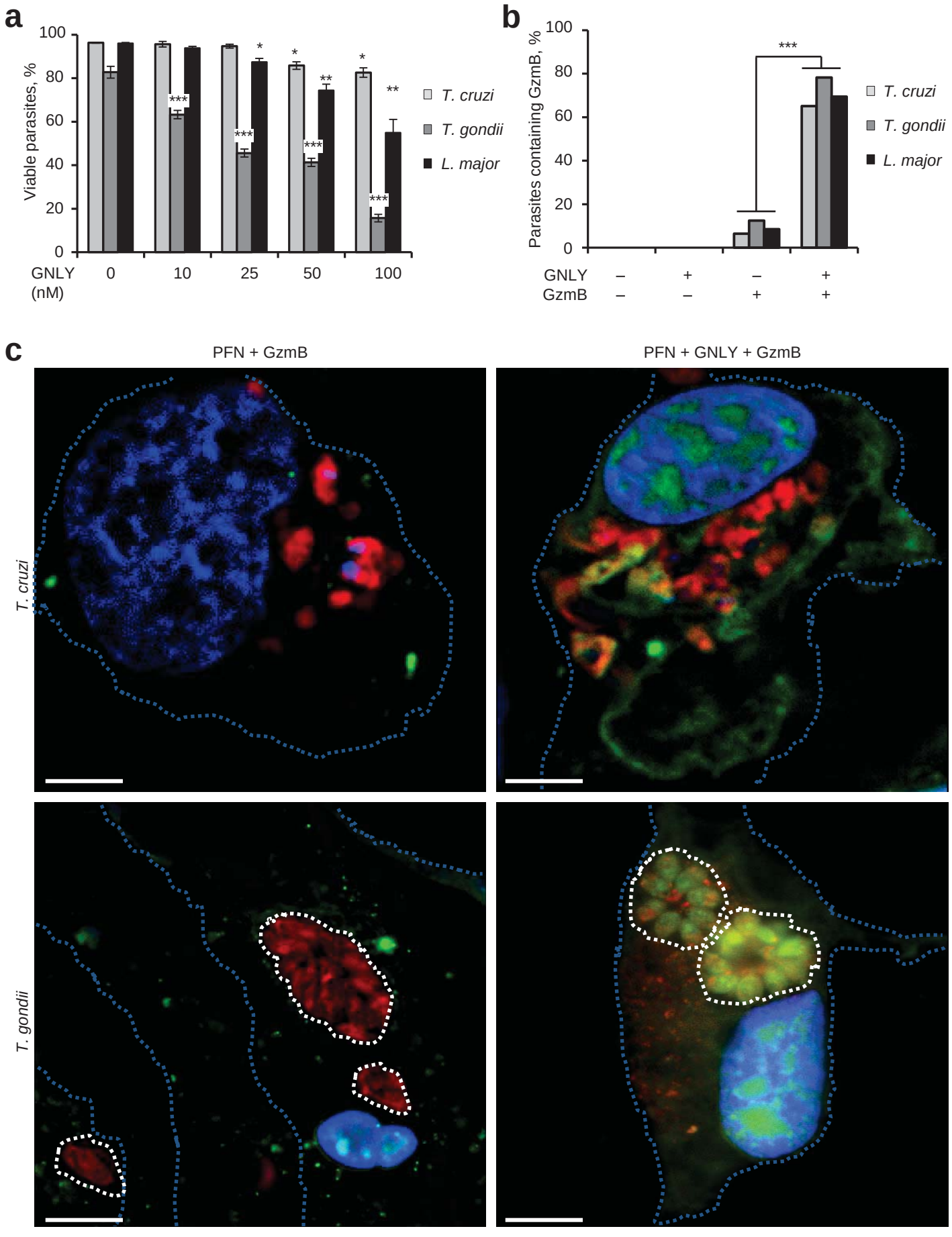

Supplementary Figure 1: Sublytic GNLY delivers Gzms into parasites and kills them. (**a**) *T. cruzi, T. gondii* (RH strain) and *L. major* were treated with increasing concentrations of GNLY to determine the sublytic concentration, the lowest GNLY concentration that causes 10–20% lethality compared to untreated parasites. Shown are mean±SEM of 3 experiments. P values calculated by unpaired Student's t–test compared to no GNLY (***, *P<0.001;* **, *P<0.01;* *, *P<0.05*). (**b**) 300–500 cell images from 50 microscopy fields for each condition were analyzed for GzmB internalization by line intensity analysis as in (Fig. 1). P values were calculated by Chi–squared test, comparing GNLY + GzmB treatment to GzmB alone (***, *P<0.001*). (**c**) Magnified view of Figure 1b merged channels. DDAO–se stained *T.cruzi* infected LLC–MK2 cells and mCherry–expressing *T.gondii*–infected HFF cells were treated with PFN and GzmB–488 with or without GNLY. Parasites are red, GzmB–488 is green and cell nuclei (DAPI staining) are blue. Parasitophorous vacuoles and host cell plasma membrane outlined with white and blue dotted lines, respectively. Scale bar, 10 μm.

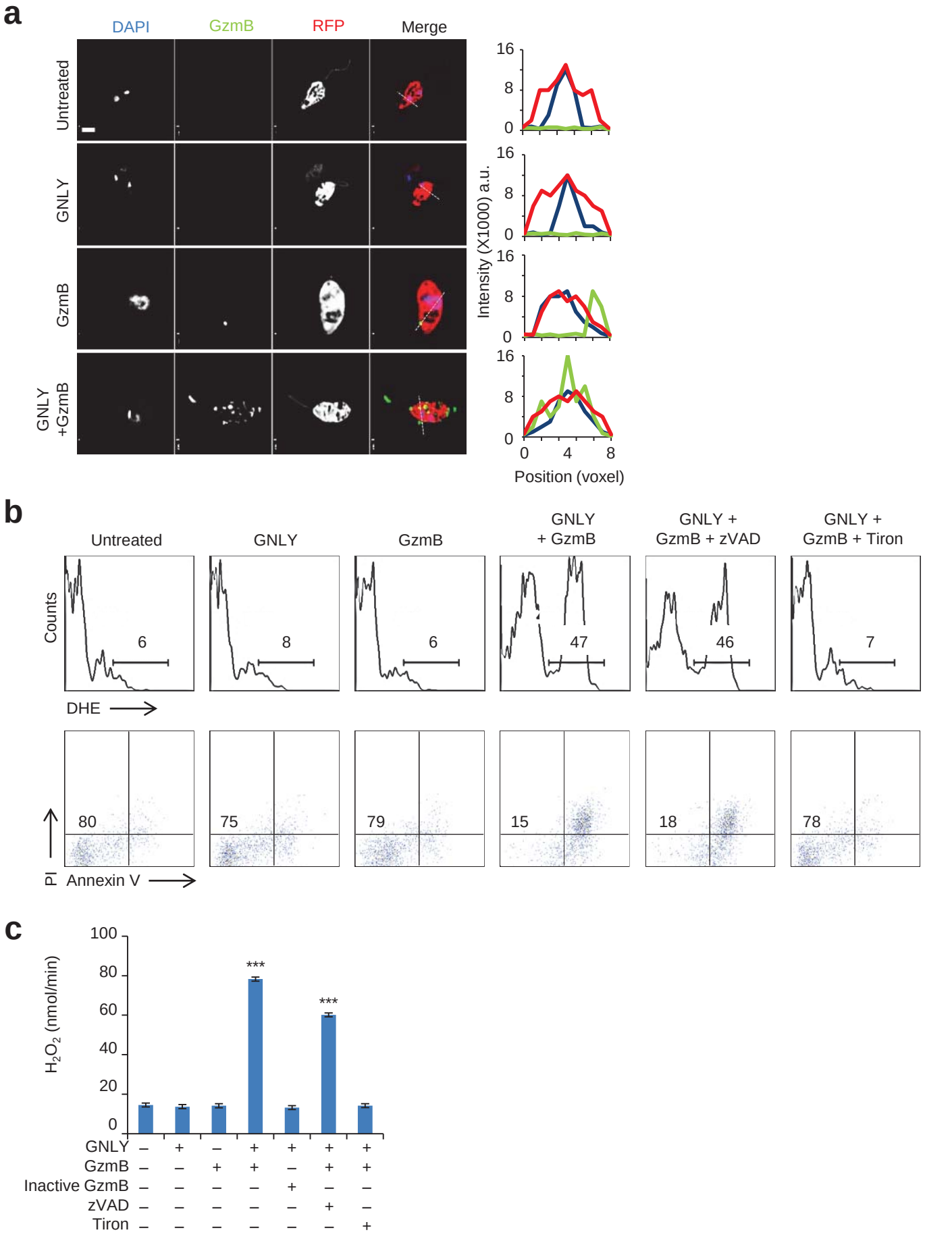

Supplementary Figure 2: GNLY delivers GzmB into extracellular *L. major* and kills them in an ROS–dependent manner. (**a**) RFP–expressing *L. major* promastigotes were untreated or treated with sub–lethal GNLY and/or inactive GzmB–488 for 30 min before analysis by fluorescence microscopy. Channel intensities along an arbitrary line across the parasite are shown at right. Scale bar, 1 μm. Representative images of 3 independent experiments are shown (a.u. – arbitrary unit). (**b**) DHE fluorescence (top) and Annexin V/PI staining (bottom) of *L. major* parasites treated for 30 min with GNLY and/or GzmB. Numbers indicate percent of DHE fluorescent cells (top) or percent viable parasites (bottom). zVAD–fmk or Tiron were added to some wells as indicated. Representative flow cytometry data of 3 independent experiments are shown. (**c**) Rate of H_2O_2 production by Amplex–Red assay over 2 hr after adding GNLY and/or active or inactive GzmB. Some samples were pre–treated with Tiron or zVAD–fmk. Mean±SEM of 3 independent experiments is shown (***, *P<0.001* compared to untreated cells by one way ANOVA).

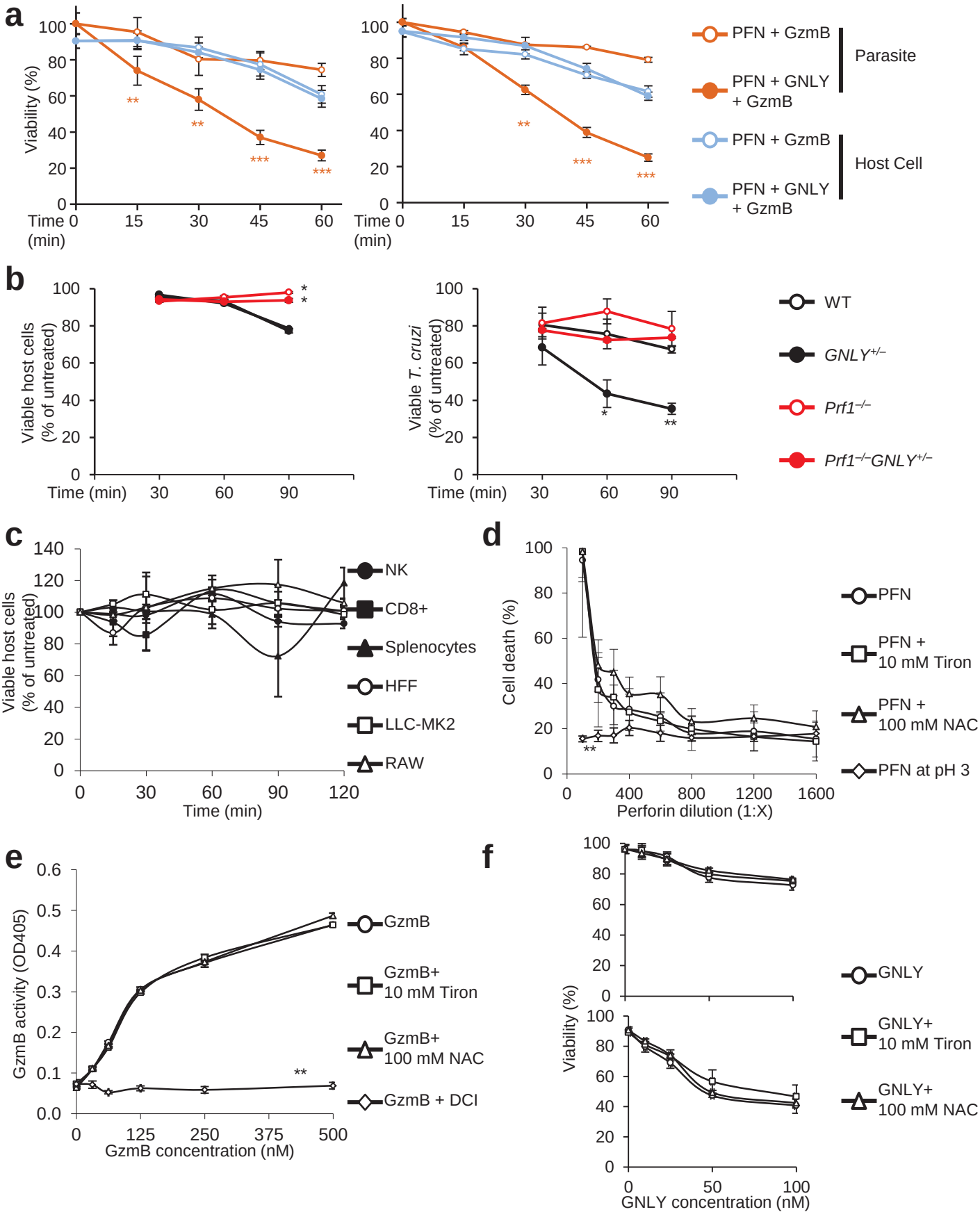

Supplementary Figure 3: PFN, GNLY and GzmB together kill intracellular parasites. (**a**) Kinetics of killing of *T. cruzi* (left), *T. gondii* (right) and their host cells. Parasite viability was assessed after 1 h by motility and plaque assay, respectively, and host cell viability was measured by 4 h ^{51}Cr release assay. (**b**) Splenocytes from *T. cruzi*–infected WT, *GNLY*$^{+/-}$, *Prf1*$^{-/-}$ or *Prf1*$^{-/-}$*GNLY*$^{+/-}$ mice were incubated with *T. cruzi*–infected, anti–CD3–coated RAW 264.7 cells at an effector : target ratio of 5:1 for indicated times. Host cell viability (left) was assessed by 4 h ^{51}Cr–release assay. Viable parasites (right) were counted in parallel cultures after 3 d. (**c**) Incubation with 250 μM DCI for 2 hr is not cytotoxic. Mouse NK, CD8+ or total splenocytes and target cells used in this study (HFF, LLC–MK2, RAW cells) were incubated with DCI for indicated times and cell viability was measured by CellTiter–Glo®. Buffered Tiron (10 mM) and NAC (100 mM) (pH7.5) did not affect the activity of PFN (**d**), GzmB (**e**) or GNLY (**f**). PFN activity was tested by RBC lysis; GzmB activity was tested by 7–AAD cleavage assay; and GNLY activity was tested by measuring viability of treated extracellular *T.cruzi* (top) and *T.gondii* (bottom). Mean±SEM of 3 independent experiments is shown (***, *P<0.001;* **, *P<0.01;* *, *P <0.05* by one way ANOVA compared to the sample without Tiron or NAC. pH3 was used as a positive control to inhibit PFN and DCI was used to inhibit GzmB).

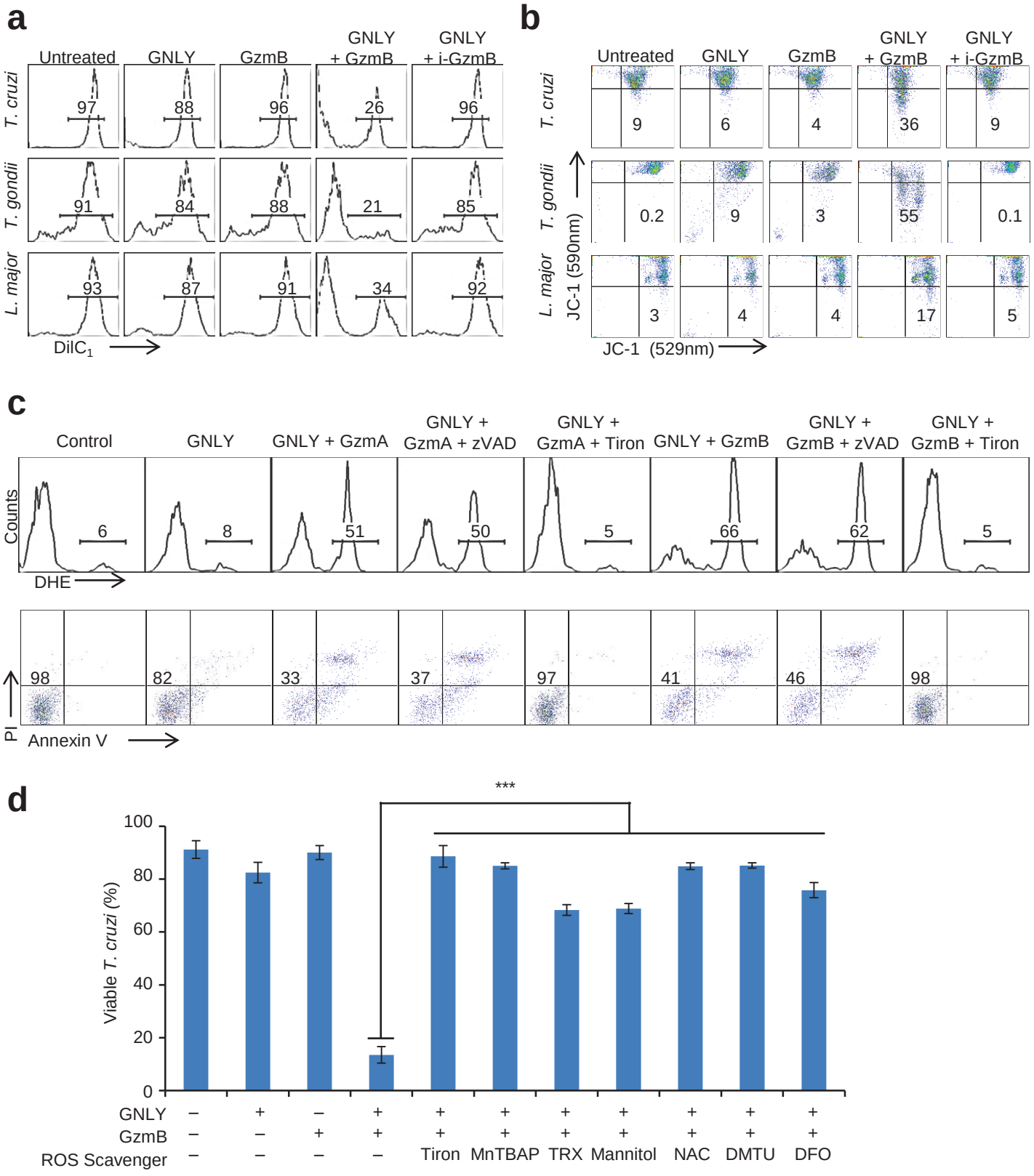

Supplementary Figure 4: Killing of extracellular parasites depends on GNLY and active GzmA or B and is inhibited by ROS scavengers, but not by a caspase inhibitor. (**a,b**) Mitochondrial membrane potential was measured by loss of $DilC_1$ fluorescence (**a**) or loss of JC–1 red fluorescence (**b**). Numbers in (**a**) indicate the percent of cells with intact mitochondrial potential and in (**b**) indicate the percent of cells that have lost transmembrane potential. Parasites were treated with GNLY and/or active or inactive (i–) GzmB for 30 or 60 min. Representative flow cytometry results from 3 independent experiments are shown. **c,** *T. cruzi,* treated for 60 min with GNLY and/or GzmA or GzmB in the presence or absence of zVAD–fmk or Tiron, were analyzed for superoxide production by DHE fluorescence (top) and for Annexin V/PI staining (bottom) by flow cytometry. Representative flow cytometry results from 3 independent experiments are shown. Numbers on top row indicate % of cells with DHE staining and on bottom row, % viable cells (Annexin V–PI–). (**d**) *T.cruzi* death from GNLY and GzmB, measured by AnnexinV/PI staining, is rescued by ROS scavengers Tiron, manganese (III) tetrakis 4–benzoic acid porphyrin chloride (MnTBAP), Trolox (TRX), mannitol, N–acetyl cysteine (NAC), dimethylthiourea (DMTU) and desferroxamine mesylate (DFO). Mean±SEM of 3 independent experiments is shown (****, P<0.001; *, P<0.05* compared to cells treated in the absence of ROS scavengers by one way ANOVA).

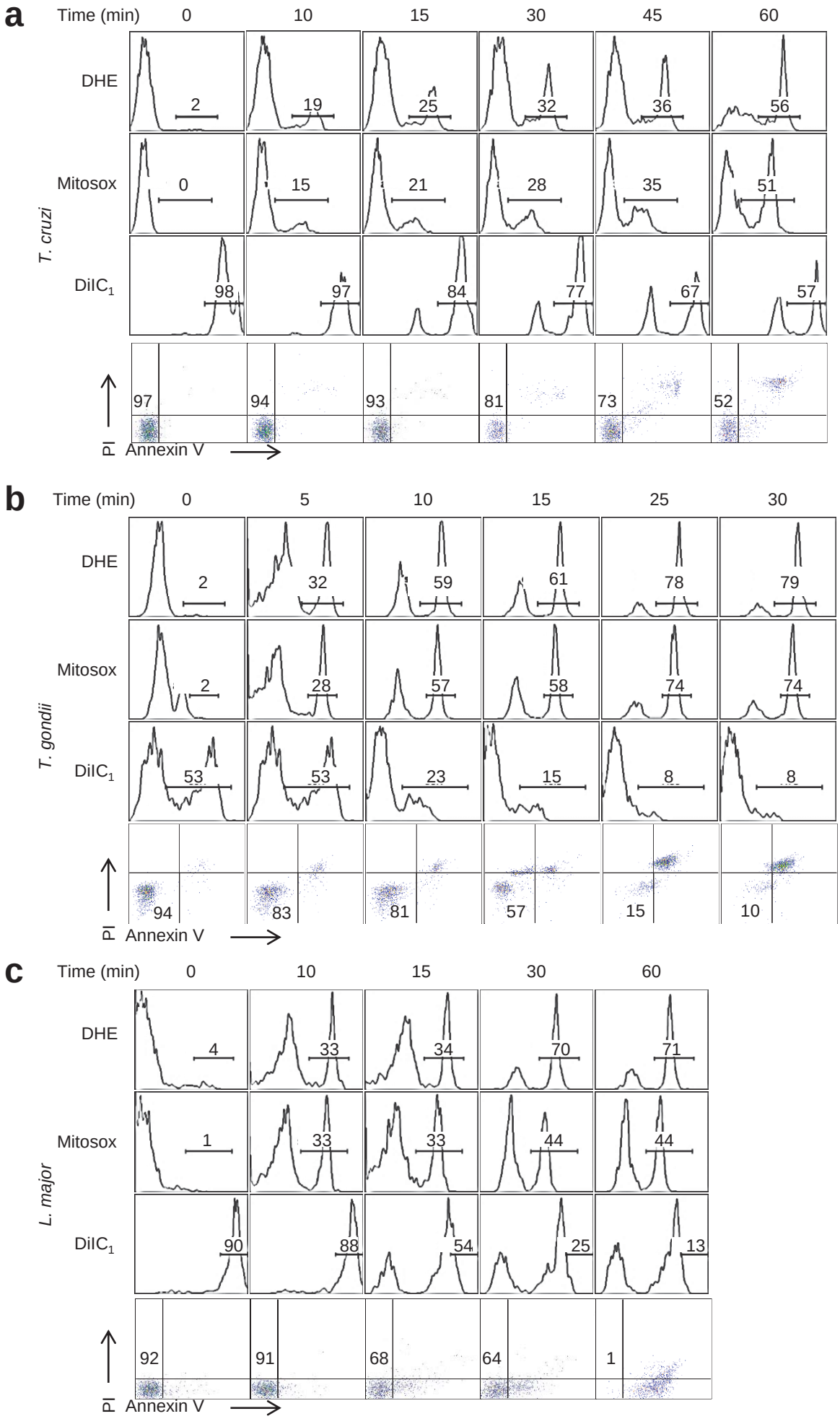

Supplementary Figure 5: Kinetics of GzmB–mediated parasite death. *T. cruzi* (**a**), *T. gondii* (**b**), and *L. major* (**c**) were treated with GNLY and GzmB in a time course experiment. Superoxide (DHE), mitochondrial superoxide (Mitosox), mitochondrial membrane potential ($DiIC_1$) and cell death (Annexin V/PI) were measured by flow cytometry at indicated times after treatment. The numbers in the DHE and Mitosox graphs represent percent of cells with superoxide fluorescence, while in $DiIC_1$ graphs show percent of cells with maintained mitochondrial potential. The numbers in Annexin/PI graphs indicate the percent of viable cells. Results show representative data from 3 independent experiments.

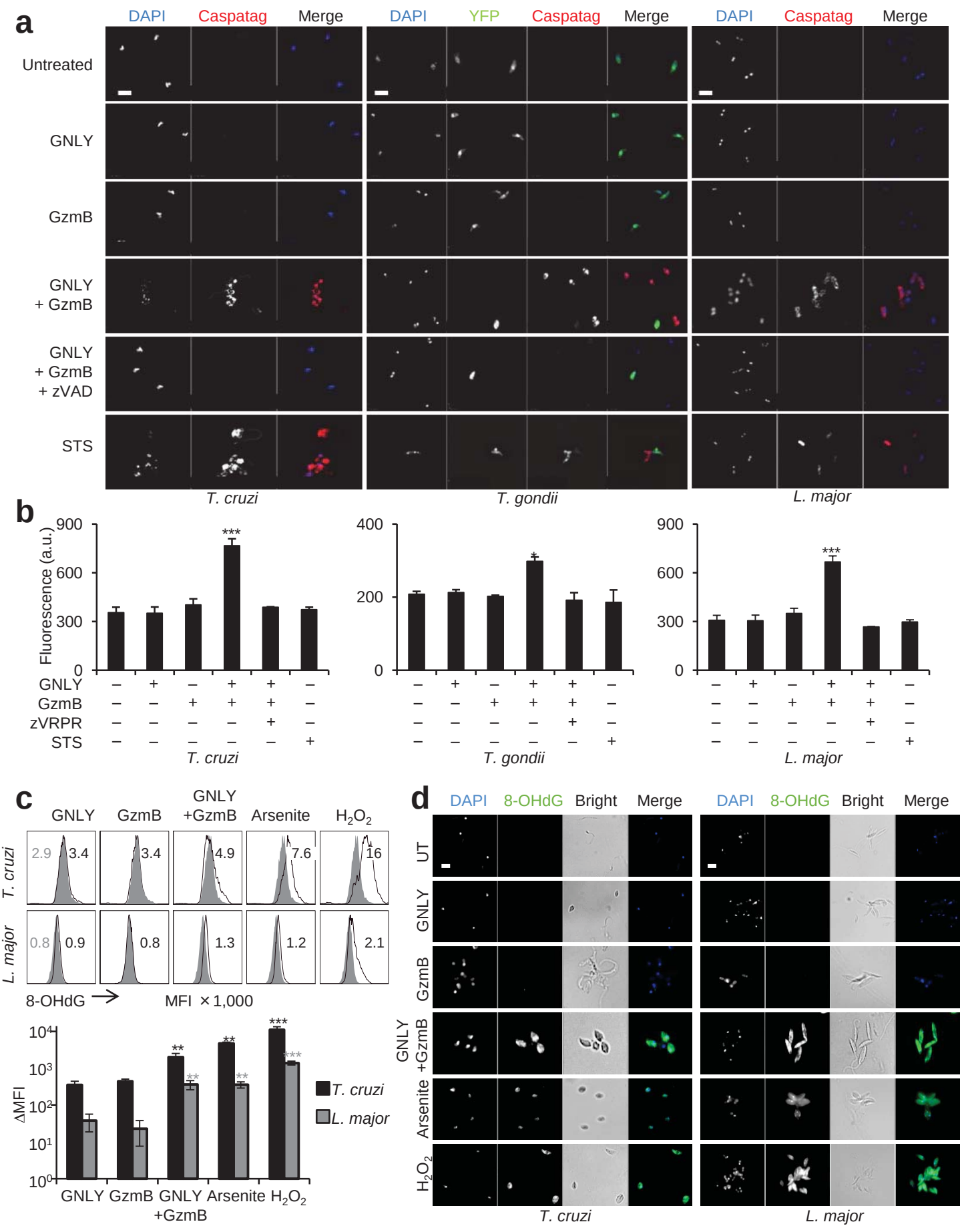

Supplementary Figure 6: GzmB treatment activates caspase–like and metacaspase activity and causes oxidative DNA damage in parasites. (**a**) *T. cruzi*, YFP–expressing *T. gondii*, and *L. major* were labeled with CaspaTag™, an indicator of active caspases, and treated with GNLY and/or GzmB or staurosporine (STS). In some wells the caspase inhibitor zVAD–fmk was added. Some *T. gondii* cells with caspase–like activity staining lose YFP fluorescence because the protein leaks from dying cells. Scale bar, 10 μm. (**b**) Ac–VRPR–AMC fluorescence, an indicator of metacaspase activation, was measured 2 h after adding GNLY and/or GzmB or STS. The pan–metacaspase inhibitor zVRPR–fmk was added to indicated wells (a.u. – arbitrary unit). (**c,d**) 8–oxoguanine (8-OHdG), a product of oxidative DNA damage, was assessed by flow cytometry (**c**) and confocal microscopy (**d**) 1 h after adding GNLY and/or GzmB or the oxidants arsenite or H_2O_2. Scale bar, 5 μm. UT, untreated. In (**c**, top) flow cytometry histogram for treated parasites (black line) is compared with untreated parasites (gray). Mean fluorescence intensity (MFI) of treated parasites is shown in black numbers and of untreated parasites is in gray in the lower panel. Mean±SEM in (**b**) and mean change in MFI (±SEM) in (**c**) of 3 independent experiments is shown (***, *P<0.001*; **, *P<0.01*; *, *P<0.05* compared to untreated parasites by one way ANOVA).

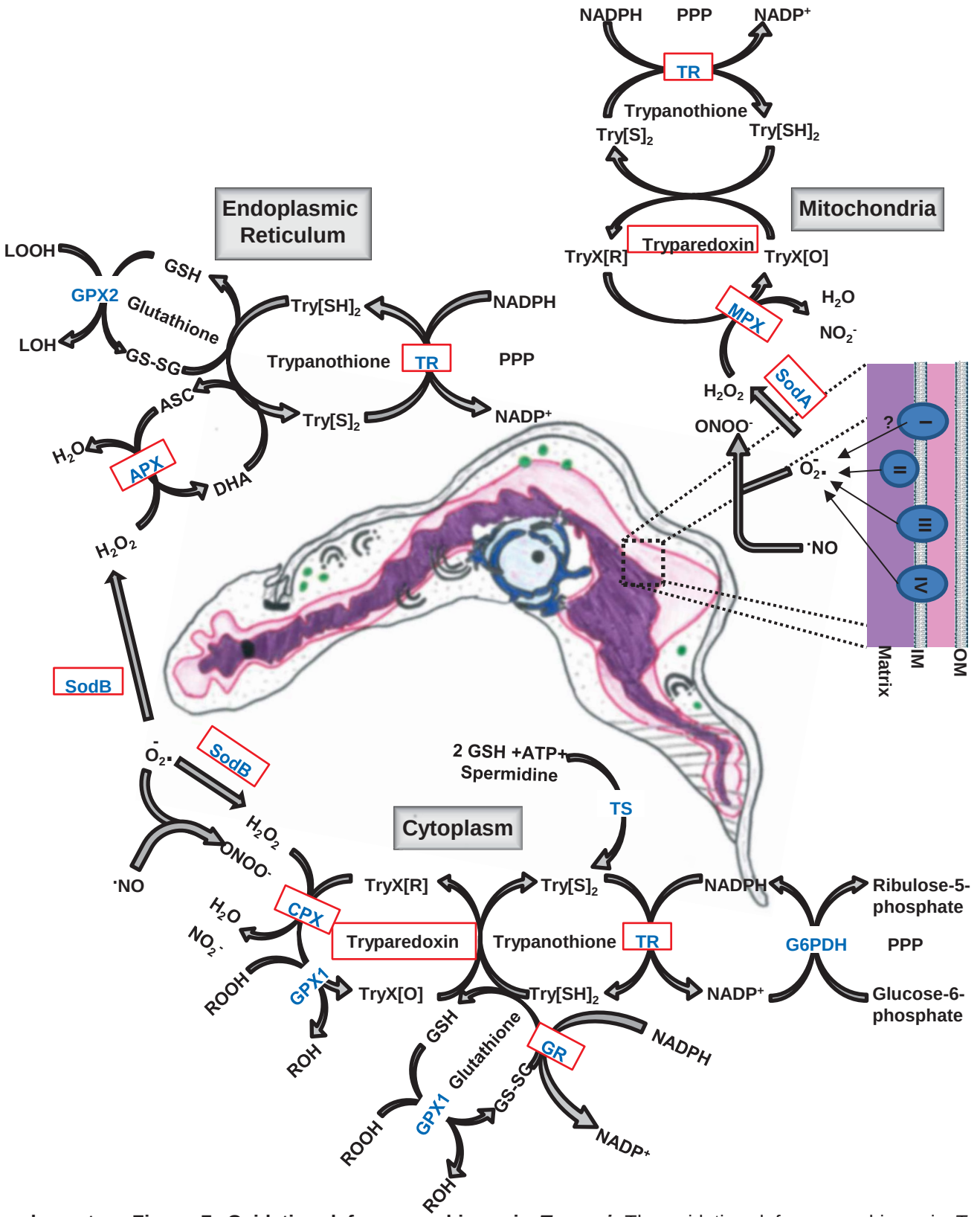

Supplementary Figure 7: Oxidative defense machinery in *T. cruzi*. The oxidative defense machinery in *T. cruzi* includes enzymes (blue) and redox substrates (black) in the endoplasmic reticulum (ER), mitochondrion, and cytosol. The final electron donor for all the enzymatic systems is NADPH produced in the pentose phosphate pathway (PPP). Reducing equivalents are funneled through the trypanothione ($Try[SH]_2$), glutathione (GSH), ascorbate (ASC), and/or tryparedoxin (TryX) redox systems. In the ER, hydrogen peroxide (H_2O_2) is metabolized by ascorbate–dependent peroxiredoxin (APX) using ASC as the electron donor, to form dehydroascorbate (DHA) which is reduced by direct reaction with $Try[SH]_2$. In the presence of redox–active metals, H_2O_2 reacts with lipids to generate lipid hydroperoxides (LOOH), which are substrates of GSH–dependent peroxidase II (GPX2). $Try[SH]_2$ also reduces oxidized glutathione (GSSG) to GSH, while trypanothione reductase (TR) reduces oxidized trypanothione ($Try[S]_2$). In mitochondria, the electron transport chain (ETC) (II: succinate dehydrogenase; III: ubiquinol–cytochrome c reductase and IV: cytochrome c oxidase) is the principal site of superoxide ($O_2^{\cdot-}$) formation, mainly at ETC III. ETC I is not well defined in *T. cruzi*. Mitochondrial superoxide dismutase (SodA) catalyzes the dismutation of $O_2^{\cdot-}$ to H_2O_2. In the presence of $O_2^{\cdot-}$, host–derived nitric oxide •NO forms peroxynitrite $ONOO^-$. Mitochondrial peroxiredoxin (MPX) reduces H_2O_2 or $ONOO^-$ using reduced TryX (TryX[R]) and $Try[SH]_2$. In the cytosol, H_2O_2 or $ONOO^-$ can react with and damage proteins to form alkyl hydroperoxides (ROOH). Antioxidant enzymes in the cytosol include cytosolic peroxiredoxin (CPX), SodB, and GPX1. $Try[SH]_2$ is synthesized from GSH and spermidine in a reaction catalyzed by trypanothione synthase (TS). The glutathione redox system uses GSH, which is reduced from GSSG by glutathione reductase (GR). The oxidative branch of the PPP provides reducing equivalents from NADPH. Validated targets of GzmB (Fig. 2f) are shown in red boxes.

Dotiwala Supplementary Figure 7

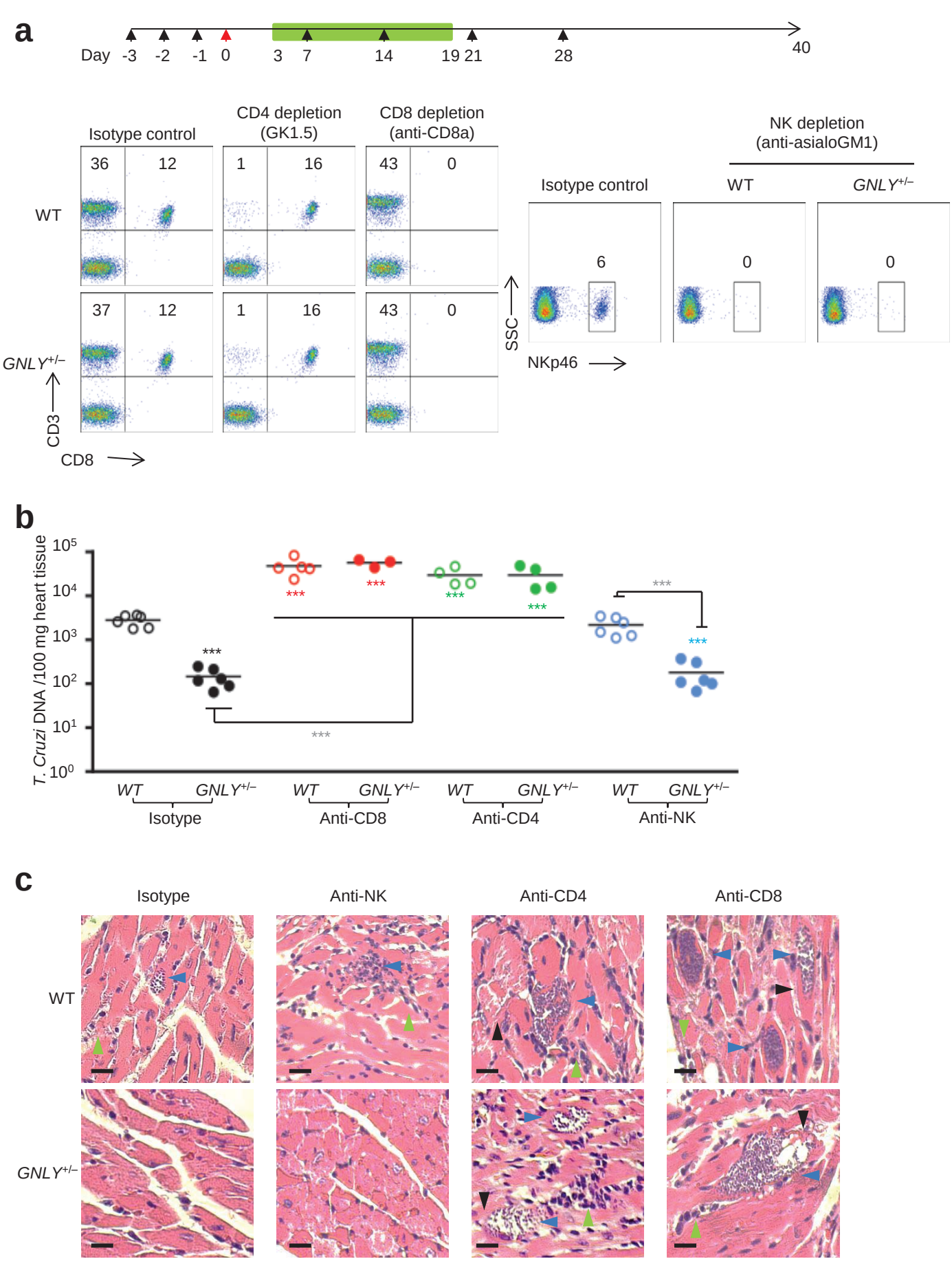

Supplementary Figure 8: Resistance of *GNLY*$^{+/-}$ mice to *T. cruzi* infection is mostly mediated by CD8+ T cells. (**a**) Experimental schema. WT and *GNLY*$^{+/-}$ mice were depleted of CD8 or CD4 T cells or NK cells by intraperitoneal (IP) injection of specific or control antibody at days indicated by black arrows. On day 0 (red arrow), mice were infected IP (*n=8*) and parasitemia assessed on alternate days between day 3 and day 19 (green bar). Mice were followed for 40 d post infection for survival. Survival and parasitemia data are shown in Fig. 3e. Antibody depletion was verified by flow cytometry analysis of blood mononuclear cells on day –1. Representative flow cytometry analysis is shown. (**b**,**c**) Mice (*n=3–6*) treated as above were sacrificed on d 18 after infection and cardiac parasite load assessed by PCR for *T. cruzi* DNA relative to mouse DNA (**b**) and by H&E staining (**c**). Statistical differences compared to control IgG–treated WT mice, or between the indicated groups (***, P<0.001; **, P<0.01*; calculated by one way ANOVA test). In (**c**) parasite–infested muscle cells (blue arrow), infiltrating inflammatory cells (green arrow) and necrotic muscle cells (black arrow) are indicated. Scale bar, 20 μm.